ANTIOXIDANTS & REDOX SIGNALING
Volume 14, Number 8, 2011

DOI: 10.1089/ars.2010.3410

ORIGINAL RESEARCH COMMUNICATION

Functional Analysis of Novel Analogues of E3330 That Block the Redox Signaling Activity of the Multifunctional AP Endonuclease/ Redox Signaling Enzyme APE1/Ref-1

Mark R. Kelley,[1–3] Meihua Luo,[1] April Reed,[1] Dian Su,[4] Sarah Delaplane,[2] Richard F. Borch,[5] Rodney L. Nyland II,[5] Michael L. Gross,[4] and Millie M. Georgiadis[2,6]

Abstract

APE1 is a multifunctional protein possessing DNA repair and redox activation of transcription factors. Blocking these functions leads to apoptosis, antiangiogenesis, cell-growth inhibition, and other effects, depending on which function is blocked. Because a selective inhibitor of the APE redox function has potential as a novel anticancer therapeutic, new analogues of E3330 were synthesized. Mass spectrometry was used to characterize the interactions of the analogues (RN8-51, 10-52, and 7-60) with APE1. RN10-52 and RN7-60 were found to react rapidly with APE1, forming covalent adducts, whereas RN8-51 reacted reversibly. Median inhibitory concentration (IC_{50} values of all three compounds were significantly lower than that of E3330. EMSA, transactivation assays, and endothelial tube growth-inhibition analysis demonstrated the specificity of E3330 and its analogues in blocking the APE1 redox function and demonstrated that the analogues had up to a sixfold greater effect than did E3330. Studies using cancer cell lines demonstrated that E3330 and one analogue, RN8-51, decreased the cell line growth with little apoptosis, whereas the third, RN7-60, caused a dramatic effect. RN8-51 shows particular promise for further anticancer therapeutic development. This progress in synthesizing and isolating biologically active novel E3330 analogues that effectively inhibit the APE1 redox function validates the utility of further translational anticancer therapeutic development. *Antioxid. Redox Signal.* 14, 1387–1401.

Introduction

Cellular response to DNA base damage is a highly regulated, complex biologic process. APE1/Ref-1 (also called HAP-1 or APEX, and here referred to as APE1) is a vital protein that acts both as a DNA-repair enzyme and as a redox signaling molecule, contributing to genomic maintenance in mammals. Since it was identified in 1991 as a DNA-repair enzyme and, in 1992, as a reduction-oxidation (redox) factor, APE1 has been the subject of more than 350 articles. Specifically, APE1 is a dual-function protein: (a) the major apurinic-apyrimidinic endonuclease in base excision repair (BER) pathways of DNA lesions, and (b) a redox factor regulating eukaryotic gene expression. Although most research has focused on its DNA-repair function, more-recent work has involved characterizing its redox function (1, 9, 11, 17, 18, 28, 36–40).

APE1 is a redox coactivator of many transcription factors, including the early growth response protein-1 (Egr-1), nuclear factor-κB (NF-κB), p53, hypoxia-inducible factor (HIF-1α), CREB, AP-1, and others in different cell systems (Fig. 1) (1, 4–7, 9, 13, 27). APE1 exhibits an α,β sandwich fold that includes two pseudosymmetric central β sheets with surrounding α-helices (18, 19), comprising a single folded domain. Both the repair and redox activities reside within this domain, including residues 40–318; the N-terminal 40-amino-acid residues are disordered and are not required for either function (9, 18). Although the divalent metal ion-dependent reaction by which APE1 catalyzes cleavage of the DNA backbone 5′ of the abasic site has been detailed (20, 21), the mechanism for the redox activity has not yet been elucidated. What is known about the redox activity of APE1 is that Cys 65 is critical for the activity and that other Cys residues are likely involved (9).

Departments of [1]Pediatrics (Section of Hematology/Oncology), Herman B. Wells Center for Pediatric Research, [2]Biochemistry & Molecular Biology, and [3]Pharmacology & Toxicology; Indiana University School of Medicine, Indianapolis, Indiana.
[4]Department of Chemistry, Washington University in St. Louis, St. Louis, Missouri.
[5]Department of Medicinal Chemistry and Molecular Pharmacology and the Cancer Center, Purdue University, West Lafayette, Indiana.
[6]Department of Chemistry and Chemical Biology, Indiana University Purdue University at Indianapolis, Indianapolis, Indiana.

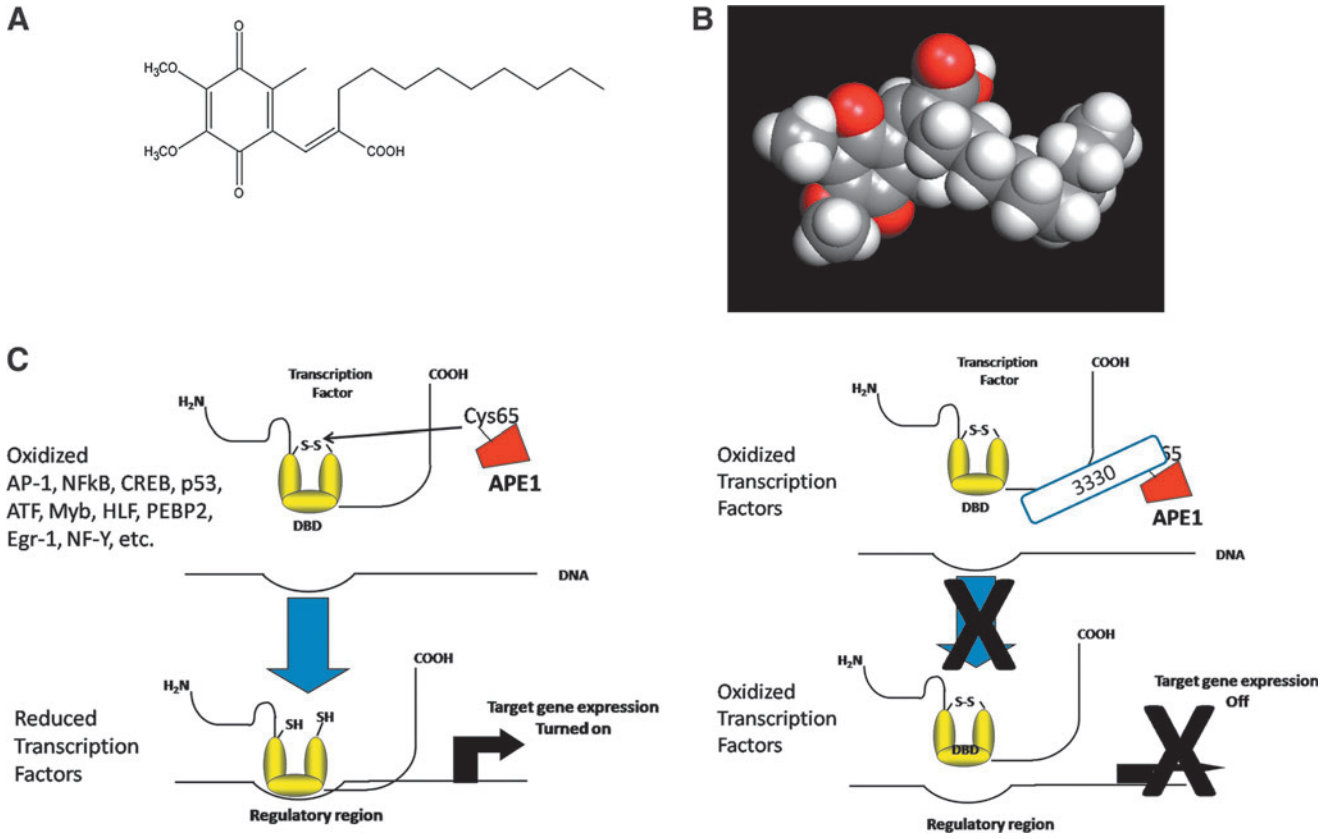

FIG. 1. Small-molecule inhibition of APE1 redox signaling activity. **(A)** Structure of E3330. **(B)** Space-filling model of E3330 was produced by using the software Vida 3.0.0 from OpenEye Scientific Software, Inc. (Santa Fe, NM; www.eyesopen.com). **(C)** APE1 interacts with downstream transcription factors (TFs) such as NF-κB, HIF-1α, CREB, FOS, JUN, and so on, converting them from oxidized to reduced states, allowing them to bind to their target promoters and switch on the transcription of genes. However, E3330 and analogues presented in this article interfere with this redox signaling by blocking the APE1 ability to convert the oxidized TF to a reduced TF, thereby keeping the target gene transcription turned off. (For interpretation of the references to color in this figure legend, the reader is referred to the web version of this article at www.liebertonline.com/ars).

We have proposed that the redox activity of APE1 involves an alternate conformation of the enzyme (9, 18).

APE1 demonstrates altered levels of expression in many cancers, including pancreatic, multiple myeloma, breast, prostate, ovarian, cervical, germ cell tumors, gliomas, osteosarcomas, rhabdomyosarcomas, and non–small cell lung cancer (2, 12, 14, 23–25, 29, 35). High APE1 expression is associated with chemo/radiotherapy resistance, poor outcomes, incomplete therapeutic responses, shorter relapse-free intervals, shorter survival times, and accelerated angiogenesis (2, 12, 14–28). Reduced levels of APE1 in pancreatic lines alter HIF-1α activity and increase sensitivity to gemcitabine (16, 38, 39). Therefore, inhibition or alteration of the APE1 function—particularly its redox function—in cancer cells can affect both tumor cell growth and the tumor microenvironment (17, 18, 38, 39).

To isolate and study the role of redox regulation by APE1 in cancer cells, we have available to us a novel quinone derivative, E3330 (Fig. 1) (10, 19, 22, 26). While searching for NF-κB inhibitors, it was determined that E3330 is highly selective in inhibiting APE1 redox function and blocking the ability of APE1 to convert various transcription factors (TFs) from an oxidized, inactive state to a reduced, active state (Fig. 1) (10). Far-Western blots and binding assays between radiolabeled E3330 and proteins renatured on membrane blots demonstrated that ^{14}C-labeled E3330 selectively bound to both recombinant APE1 and purified APE1 from cell nuclear extracts (26).

Presently only a few compounds reportedly inhibit APE1 redox activity: E3330 and a series of quinones that exhibit micromolar inhibition (22). From the many benzoquinone and naphthoquinone analogues of the APE1-inhibitor E3330 that were synthesized (22), three stand out as having the most interesting potential for biologic studies and as providing the clearest demarcation for a structure–activity relation (SAR) approach to new analogue development; their properties are described here. They were designed and synthesized to explore (a) inhibition of cell growth, and (b) structural changes caused by redox regulation, the major biologic effect of inhibiting APE1 redox activity (17, 22). Additionally, redox inhibitors can be used as therapeutics or novel tools for separating the APE1 DNA-repair activity from its redox function in *in vitro* and cellular studies.

Materials and Methods

Reagents

E3330 and its analogues (RN8-51, RN10-52, and RN7-60) were synthesized as previously described, as was RN7-58 (17, 22). Resveratrol was purchased from Sigma-Aldrich (St. Louis, MO).

Expression and purification of proteins

Human APE1 delta 40 proteins were expressed and purified as previously described (9). Site-directed mutagenesis with the Stratagene Quikchange kit (La Jolla, CA) was used to introduce C99A, C138A, and C99A/C138A substitutions in APE1 delta 40. Substituted APE1 delta 40 proteins were expressed and purified as described for APE1 delta 40 and confirmed by DNA sequencing analysis.

To express and purify full-length APE1 (FL-APE1), an N-terminal hexa-His- SUMO-fusion (Invitrogen, Rockville, MD) was constructed. The fusion construct was transformed into Rosetta (DE3) *Escherichia coli* (Novagen, Gibbstown, NJ), grown in 3 L of LB media with 20 μg/ml kanamycin and 34 μg/ml chloramphenicol until the OD at 600 nm reached 0.6, and then induced overnight with 1 m*M* isopropyl thiogalactoside at 15°C. The cultures were harvested by centrifugation at 4,000 *g* for 30 min, and the pellets were stored at −80°C. Each cell pellet was resuspended in 20 ml of 50 m*M* sodium phosphate buffer, pH 7.8, 0.3 *M* NaCl, 10 m*M* imidazole, and then lysed by using a French press (SLM-AMINCO; Spectronic Instruments, Rochester, MN) at 1,000 psi. The suspension was centrifuged at 35,000 rpm for 35 min, and the supernatant was then loaded on an Ni-NTA column at 4°C. The column was washed with 20 column-volumes of 50 m*M* sodium phosphate buffer, pH 7.8; 0.3 *M* NaCl, 20 m*M* imidazole protein, and then incubated overnight with the SUMO-specific protease Ulp1 added at a molar ratio of ~1:1,000 (Ulp1/FL APE1). Full-length APE1 was then eluted from the column in the same buffer and further purified by using an S-Sepharose column (GE Healthcare, Piscataway, NJ) run in 50 m*M* MES, pH 6.5, 1 m*M* DTT, and a linear NaCl gradient (0.05–1 *M*). The peak fractions were then combined, concentrated, and subjected to gel filtration chromatographic separation by using a Superdex 75 (GE Healthcare) in 50 m*M* Tris, pH 8.0, 0.1 *M* NaCl. Fractions containing full-length APE1 were then concentrated by using Amicon Ultra centrifugal concentrators (Millipore, Billerica, MA) and stored at −80°C.

Cloning, protein expression, and purification of human thioredoxin. The gene encoding human thioredoxin (TRX) was cloned into pET15b vector with restriction endonucleases *Nde*I and *Bam*HI and confirmed by DNA sequencing. Protein was expressed in *E. coli* Rosetta after induction with 1 m*M* isopropyl β-D-thiogalactoside (IPTG) induction overnight at 18°C. The cells were harvested by centrifugation and frozen at −80°C. Frozen cells were thawed and resuspended in lysis buffer (50 m*M* phosphate buffer, pH 7.8, 0.3 *M* NaCl, 10 m*M* imidazole) and lysed by using a French press. The recombinant protein was purified by Ni-nitrilotriacetic acid (Ni-NTA) column chromatography and Q-sepharose column chromatography in 50 m*M* Tris-HCl, pH 8.5, with a linear NaCl gradient. Thrombin was added to the eluted sample overnight at 4°C to remove the N-terminal histidine tag, resulting in human TRX protein with three extra amino acids G-S-H at its N-terminal. The protein was finally purified by Q-sepharose column chromatography in 50 m*M* Hepes, pH 7.5, with a linear NaCl gradient. The final product is one band on SDS-PAGE.

APE1-repair assays. Oligonucleotide gel-based APE1 endonuclease activity assays were performed as previously described (6, 15).

Cell-survival/killing assays. The 3-(4, 5-dimethylthiazol-2-yl)-5-(3-carboxymeyhoxyphenyl)-2-(4-sulfophenyl)-2H-tetrazolium (MTT) dye assays for cell growth were performed as previously described (6, 32).

Mass Spectrometric Analysis

Global ESI-QTOF Experiments. Protein samples were analyzed in the positive-ion mode on a Bruker MaXis UHR-TOF (ultra-high resolution time-of-flight) (Bruker Corp., Fremont, CA). Capillary voltage was set at −3,600 V. Nebulizer pressure was 0.4 bar, and dry gas was at 1.0 L/min. The drying temperature was 180°C. The instrument was calibrated by using Tuning Mix (Agilent Technologies, Santa Clara, CA) as the external mass calibrant. Spectral deconvolution was performed by using MaxEnt with Data Analysis (provided by the manufacturer of the spectrometer). Reactions of protein and redox inhibitors were carried out at a 1:5 molar ratio of protein (100 μ*M*) to ligands (500 μ*M*) in 10 m*M* HEPES (Sigma, St. Louis, MO) buffer at pH 7.5 at room temperature. Reactions were quenched on dry ice before mass spectrometry (MS) analysis. Typically, 200–300 pmol of protein samples were loaded on an Opti-Guard C18 column (10×1 mm i.d.; Cobert Associates; St. Louis, MO) for desalting and then eluted to mass spectrometer by using 50% (vol/vol) acetonitrile with 0.1% formic acid (FA) at 10 μl/min. The percentage of difference species for analysis of RN8-51 reaction with APE1 was estimated by the observed peak intensities based on the assumption that the ionization efficiency of the protein molecule is not changed by the modification.

LC-MS/MS experiments

A 10-μl solution of APE1 (100 μ*M*) and RN6-70, RN10-52, or RN8-51 (500 μ*M*) was incubated in 10 m*M* HEPES (pH 7.5) at room temperature for 0.5 h. DTT (protein/DTT = 1:20, mol/mol) was added to quench the reaction. The sample was diluted with water to a final concentration of 1 μ*M*. A portion of the final diluted solution (50 μl) was submitted to trypsin digestion (protein/trypsin = 50:1, wt/wt) at 37°C for 4 h. The solution was then analyzed with LC-MS/MS, whereby 5 μl of digestion solution was consumed for each experiment. Reversed-phase capillary LC separations were performed with an Eksigent NanoLC-1D pump (Eksigent Technologies Inc.; Livermore, CA). The reversed-phase capillary column (0.075×150 mm) was packed in house by using a PicoFrit tip (New Objective Inc., Woburn, MA) with Magic C18 resin (5-μm particles, 200 Å pore size; Michrom Bioresources Inc., Auburn, CA). The mobile phases consisted of water with 0.1% FA (A) and acetonitrile with 0.1% FA (B). Immediately after sample loading, the mobile phase was held at 98% A for 12 min. A linear gradient was performed by using 2% to 60% solvent B over a 60-min period, then to 80% solvent B over a 10-min period at 260 nl/min, followed by a 12-min re-equilibration step by 100% solvent A. The flow was directed by a PicoView Nanospray Source (PV-550; New Objective) to the LTQ Orbitrap XL mass spectrometer (Thermo Fisher Scientific Inc., San Jose, CA). The spray voltage was 1.8–2.2 kV, and the capillary voltage was 27 V. The conventional data-dependent MS/MS acquisition method was used with the Xcalibur 2.0.7 control system, in which full spectra were collected over the range of m/z 350–2,000 followed by product-ion (MS/MS) spectra of the six most abundant ions. The full mass spectra of the peptides were acquired at high

mass-resolving power (60,000 for ions of m/z 400) with the FT analyzer. The six most abundant precursor ions were dynamically selected in the order of highest to lowest intensity (minimal intensity of 1,000 counts) and subjected to collision-induced dissociation (CID) at a normalized collision energy of 35% of the maximum available. Precursor activation was performed with an isolation width of 2 Da and an activation time of 30 ms. The automatic gain control target value was regulated at 1×10^6 for FT and 3×10^4 for the ion trap, with a maximum injection time of 1,000 ms and 200 ms for the FT and the ion trap, respectively. The instrument was externally calibrated by using a standard calibration mixture of caffeine, the peptide MRFA, and Ultramark 1621 (Thermo Fisher Scientific). To identify covalent modifications, LC-MS/MS data were searched with Mascot 2.2 (Matrix Science, London, UK). Parameters used for Mascot were: enzyme, trypsin; maximum missed cleavage, 3; peptide mass tolerance, 10 ppm with one ^{13}C peak; peptide charge, +1 to +3; product mass tolerance, 0.6 Da; instrument type, default (searching for all types of b and y ions).

Redox assays

Electrophoretic mobility shift assay. Increasing amounts of E3330 or its analogues (RN8-51, RN10-52, and RN7-60) were incubated with 2 μl purified hAPE1 or thioredoxin (reduced with 1.0 m*M* DTT, then diluted to 2 μg/μl with 0.2 m*M* DTT in PBS) in EMSA reaction buffer [10 m*M* Tris (pH 7.5), 50 m*M* NaCl, 1 m*M* $MgCl_2$, 1 m*M* EDTA, 5% (vol/vol) glycerol] with a total volume of 10 μl for 30 h. Then EMSA was performed, as previously described (17).

Transactivation assays. The established, stable Skov-3X ovarian cancer cells with NF-κB Luc gene (luciferase gene with the NF-κB–responsive promoter) (Stratagene, La Jolla, CA) (17) were treated with increasing amounts of E3330 or its analogues (RN8-51, RN10-52, and RN7-60) for 40 h. The cells were lysed; then *Firefly* luciferase activities were assayed using the Luciferase Reporter Assay System (Promega Corp., Madison, WI) in a 96-well microtiter plate luminometer (Thermo Lab Systems, Franklin, MA) and were normalized to the cell numbers measured by MTT assay (5). All of the experiments were performed in triplicate and then repeated at least three times in independent experiments.

Matrigel tube-formation assay. This assay was performed as previously described (17). In brief, Matrigel (BD Biosciences) was used to coat each well (50 μl) of a precooled 96-well plate. Retinal vascular endothelial cells (RVECs) at 5,000 cells per well were seeded and incubated in EBM with 1% fetal bovine serum and 10 ng/ml basic fibroblast growth factor at 37°C for 24 h. The formation of capillary-like structures by RVECs on the basement membrane matrix (Matrigel) was quantified by counting the number of closed tube units in each well. The percentage of the tube formation to the vehicle control group was calculated for each treated group ($n=3$).

TdT-mediated dUTP-fluorescein nick-end labeling (TUNEL). The TUNEL assay allows us to determine the percentage of cells undergoing apoptosis. The reactions were performed according to the manufacturer's protocol (Roche, Indianapolis, IN). Random fields of cells were photographed under phase microscopy and scored as percentage positive cells for the terminal transferase labeling reaction.

Statistical analysis

Quantitative data were obtained from at least three independent experiments and expressed as the mean ± SD. Statistical significances of differences between two groups were determined by using Student's t test. Statistical significance is as indicated in the figure legend.

Results

New and novel E3330 analogues block APE1 redox function

We previously demonstrated that E3330, a molecule binding specifically to APE1, blocks only the redox function of APE1 and interferes with its ability to convert a variety of transcription factors from an oxidized to a reduced state, which affects their ability to bind to their target DNA and "switch on" respective genes (17, 22). E3330 has no demonstrable effect on APE1-repair endonuclease activity (17, 22). Additionally, our data (and those of others) show that E3330 blocks angiogenesis in a variety of *in vitro* and *in vivo* models (17, 38, 39), demonstrating implications for angiogenic indications, including cancers and age-related macular degeneration (17). However, we also are interested in developing new analogues of E3330, not only to achieve sub-micromolar levels of activity, but also to help us determine the mechanism(s) by which E3330 interacts with and blocks APE1 redox function, which is still unknown (17, 18).

We recently published the results of synthesizing a number of novel E3330 analogues (22); here we present data on three of the most promising compounds. In a series of experiments using EMSA, as described previously (17), we determined that analogues RN8-51, RN10-52, and RN7-60 had redox-blocking effects similar to that observed for E3330. Interestingly, the IC_{50} values for these compounds were at least 10 times lower than that of E3330 (20 μM): RN8-51 was 0.5 μM, RN10-52 was 0.75 μM, and RN7-60 was 1.5 μM, by using AP-1 as the transcription factor target complex (Fig. 2). Both RN8-51 and RN10-52 were active at the sub-micromolar level. By comparison, an important role for the quinone moiety was established through characterization of RN7-58, in which the naphthoquinone core is replaced by a dimethoxynaphthalene core. RN7-58 shows no effect on APE1 redox activity in EMSA analysis (Fig. 2D). Similarly, a previously reported inhibitor of APE1 redox activity, resveratrol, as shown in Fig. 2A, shows no inhibitory effect on APE1 redox function, even at concentrations as high as 200 μM. We did not observe any inhibitory effect of resveratrol on APE1-repair activity (data not shown).

To pursue further the specificity of E3330 and these three analogues as APE1 redox inhibitors, we also used EMSA to test the ability of the compounds to inhibit reduction of transcription factors by thioredoxin, an important cellular redox protein. Although APE1 is the relevant redox factor for AP-1 *in vivo*, thioredoxin will reduce AP-1 *in vitro* (EMSA redox assay). As demonstrated in Fig. 3, increasing amounts of E3330, RN8-51, and RN10-52 decreased the ability of APE1 to enhance AP-1 DNA-binding but did not similarly affect the thioredoxin redox activity (panels A and B). In contrast, RN7-60 affected the abilities of both APE1 and thioredoxin to enhance AP-1 DNA binding (Fig. 3C). From these data, we concluded that E3330, RN8-51, and RN10-52 specifically blocked the redox activity of APE1 but did not affect thio-

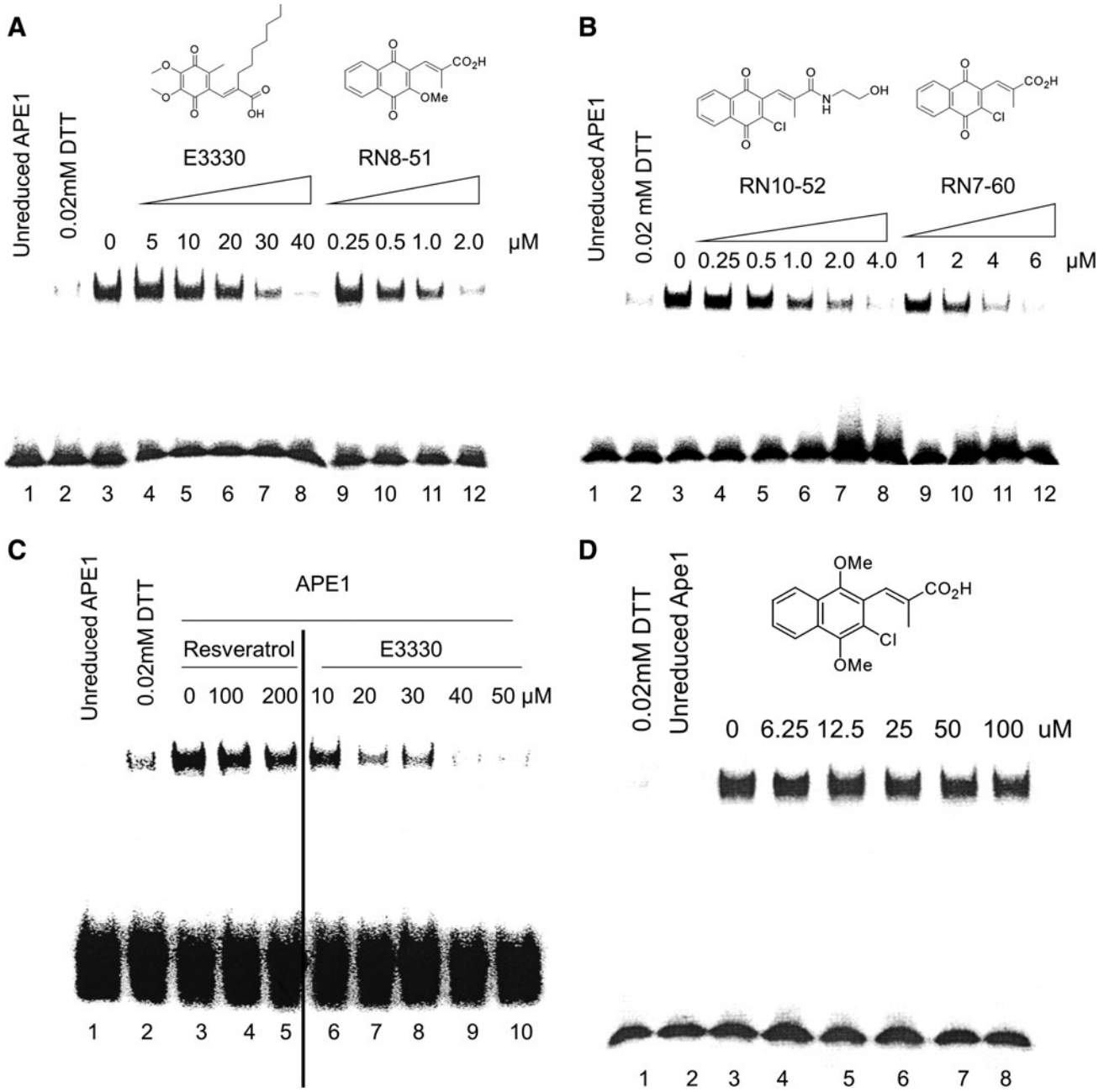

FIG. 2. E3330 analogues blocked APE1 redox function in EMSA assay. Increasing amounts of E3330 or its analogues (RN8-51, RN10-52, and RN7-60) were incubated for 30 min with 2 μl purified hAPE1 (reduced with 1.0 m*M* DTT, then diluted to 2 μg/ul with 0.2 m*M* DTT in PBS) in EMSA reaction buffer [10 m*M* Tris (pH 7.5), 50 m*M* NaCl, 1 m*M* $MgCl_2$, 1 m*M* EDTA, 5% (vol/vol) glycerol] with a total volume 10 μl. EMSA was performed with reduced APE1 and 0.02 m*M* DTT, which was the amount of DTT carried over from the reduction of APE1 as control. **(A)** RN8-51; **(B)** RN10-52, and B) RN7-60 inhibited AP-1 DNA-binding enhanced by APE1 in a dose-dependent manner, with a much lower IC_{50} (0.5, 0.75, and 1.5 μM, respectively) than E3330 (20 μM). Increasing amounts of resveratrol **(C)** or analogue RN7-58 **(D)** were incubated for 30 min with 2 μl purified human APE1 (reduced with 1.0 m*M* DTT, and then diluted to 2 μg/ul with 0.2 m*M* DTT in PBS) in EMSA reaction buffer [10 m*M* Tris (pH 7.5), 50 m*M* NaCl, 1 m*M* $MgCl_2$, 1 m*M* EDTA, 5% (vol/vol) glycerol] with a total volume 10 μl. EMSA was performed with unreduced APE1 and 0.02 m*M* DTT, which was the amount of DTT carried over from the reduction of APE1 as control. Neither compound showed any inhibitory effects. Experiments were repeated 3 times with similar results, as shown.

redoxin. RN7-60 blocked the redox activity of both, but slightly more so with APE1 than with thioredoxin. This suggests that E3330, RN8-51, and RN10-52 are specific for APE1, whereas RN7-60 appears to be a more promiscuous redox inhibitor.

Effect of E3330 and analogues on APE1-repair endonuclease function

In the past, we demonstrated that E3330 has no effect on the DNA-repair endonuclease activity of APE1 (1, 17). As shown

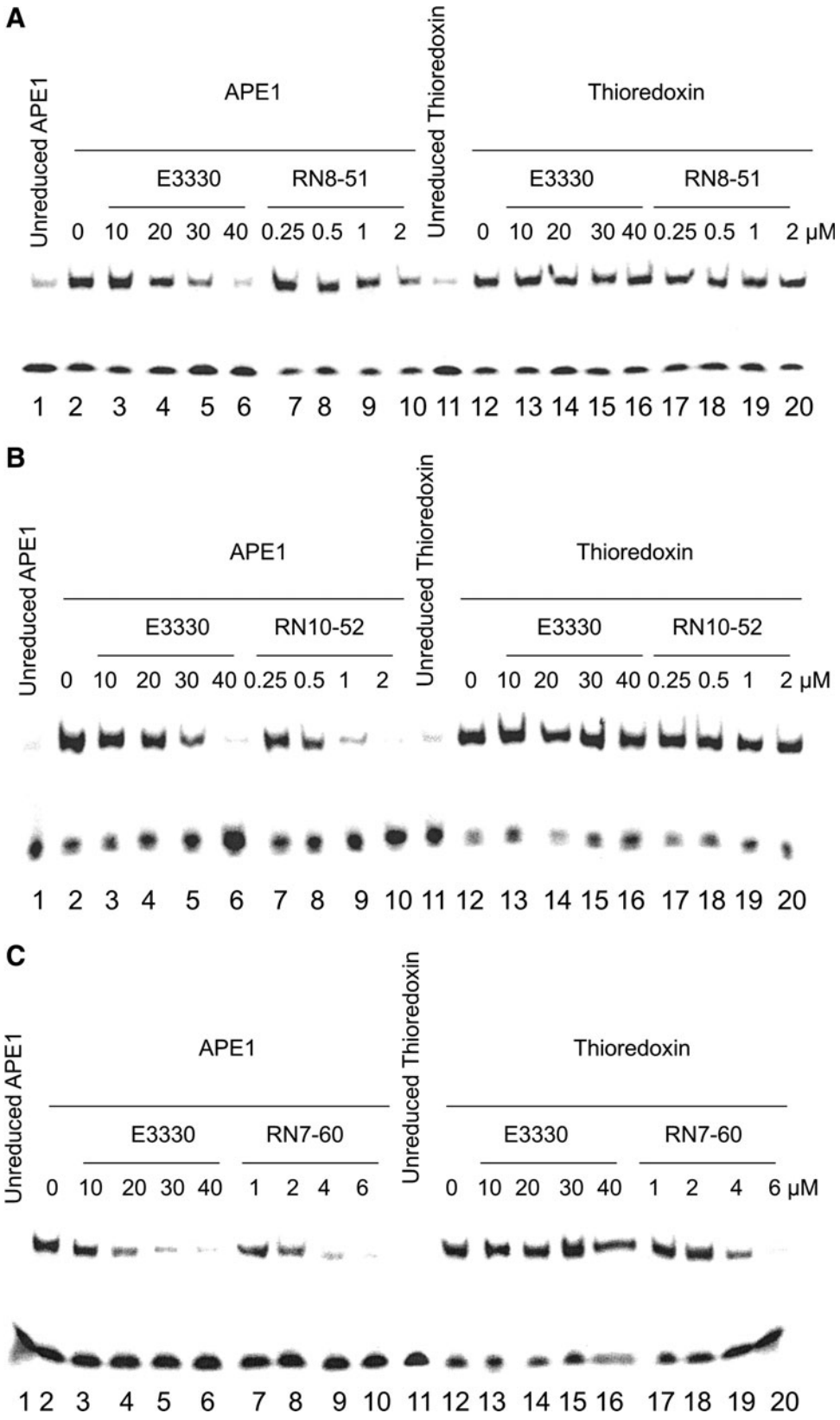

FIG. 3. Effect of E3330 analogues on APE1 and thioredoxin redox function. Increasing amounts of E3330 or its analogues (RN8-51, RN10-52, and RN7-60) were incubated for 30 min with 2 μl purified human APE1 or thioredoxin (reduced with 1.0 m*M* DTT, then diluted to 2 μg/μl with 0.2 m*M* DTT in PBS) in EMSA reaction buffer with total volume of 10 μl. The EMSA assay was performed as described in Methods. E3330 **(A–C)**, RN8-51 **(A)**, and RN10-52 **(B)** blocked the redox activity of APE1 but not thioredoxin. RN7-60 **(C)** blocked the redox activity of both, but affected APE1 more than thioredoxin.

in Fig. 4, none of the analogues blocked APE1-repair endonuclease activity, even at concentrations up to 10 times higher than those used in the EMSA experiments. These data demonstrate the specificity of these analogues for the redox—but not the repair—function of APE1.

E3330 analogues block APE1 redox signaling in cells

To determine whether the analogues will block the redox function of APE1 in cells (rather than just in cell-free assays), we investigated the ability of the analogues to block APE1 redox activity in a cell-based, transactivation assay, as used previously for E3330 (18). In this assay, an NF-κB binding sequence upstream of a luciferase reporter was stably expressed in ovarian cancer cell line SKOV-3X. Increasing amounts of E3330 and the analogues all decreased the ability of NF-κB ability to bind to the promoter (Fig. 5) in a dose-dependent manner. RN8-51, RN10-52, and RN7-60 had more than 3 times the effect that E3330 had on NF-κB activation in this assay. IC_{50} values for E3330, RN8-51, RN10-62, and RN7-60 were 80, 27, 12, and 25 μM, respectively. The results of this *in vitro* assay indicate that, in cellular studies, the analogues have the potential to block APE1 redox function more efficiently than E3330 can.

E3330 and analogues inhibit growth of ovarian cancer cell lines

Whereas APE1 plays an important role in cell growth and survival through its repair and redox functions, it is becoming apparent that the redox function of APE1 is more involved in cell growth and angiogenesis activities, whereas the repair activity is more highly attuned to cellular death (5, 17, 18, 38–40) Thus, the APE1 repair function helps prevent the triggering of apoptosis (5, 27, 28, 30), whereas APE1 protein-to-protein interactions help promote cellular proliferation. Previous studies in normal dividing cells and in neuronal cells (data not shown) do not indicate an effect of the APE1 redox function on cell survival (8, 11, 31). However, by using a cell-growth assay, we demonstrated that E3330 and the three analogues decreased the growth of both the ovarian SKOV-3X and Hey-C2 cell lines (Fig. 6). RN10-52 and RN7-60 had up to a sixfold greater inhibitory effect than E3330 did. In Skov-3X cells, the LD_{50} of RN10-52 and RN7-60 were 8.3 μM and 21.8 μM, respectively, whereas E3330 was 44.1 μM. In Hey-C2 cells; the LD_{50} values of RN10-52 and RN7-60 were 6.7 μM and 15 μM, respectively, in contrast to that of E3330,38.9 μM. RN8-51 had an effect similar to E3330: LD_{50} of 44.1 μM versus 55.9 μM in Skov-3X cells, respectively, and 40 μM versus 38.9 μM in Hey-C2 cells. These results indicate that these analogues do have cell-growth inhibitory effects on cancer cell lines.

In vitro *Matrigel tube-formation assays: angiogenesis studies*

We performed *in vitro* Matrigel tube formation assays to determine whether E3330, RN8-51, RN10-52, and RN7-60 would block endothelial tube formation, as described in Methods (Fig. 7). Early-passage (2–4 days) umbilical cord blood-derived erythroid–colony-forming units cells (ECFCs) were treated with vehicle only or with varying concentrations of E3330, RN8-51, RN10-52, or RN7-60. Low-magnification images were captured and scored to quantitate the total

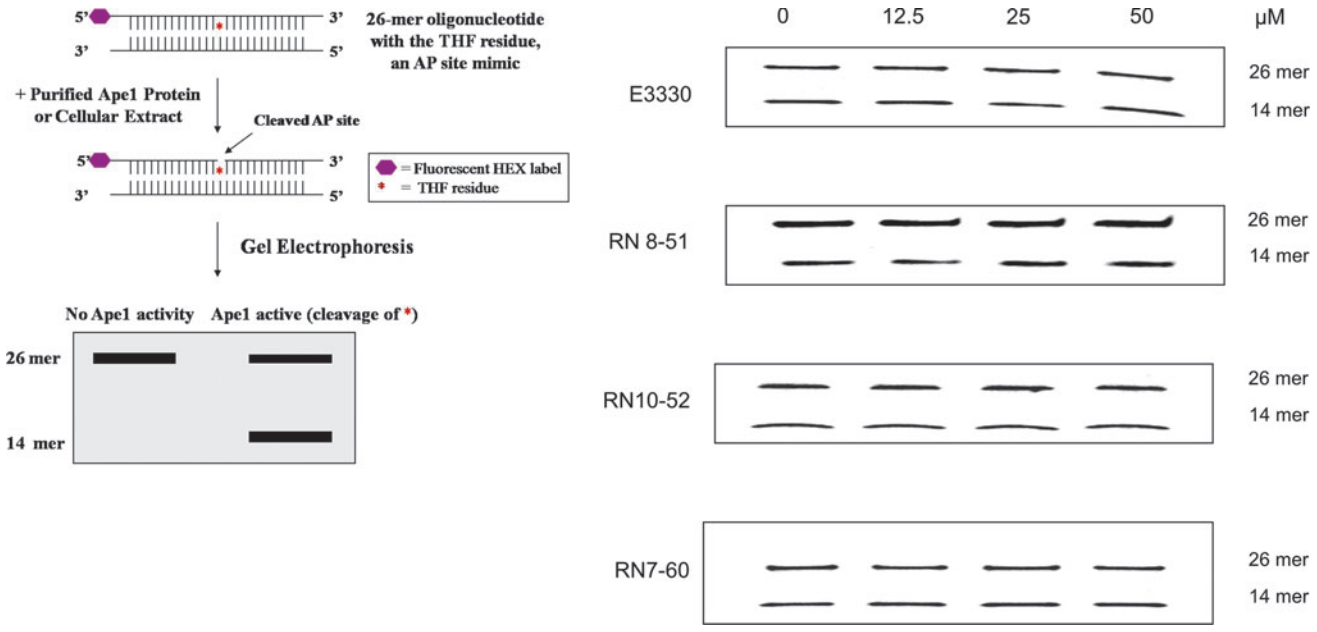

FIG. 4. Effect of E3330 analogues on APE1 endonuclease activity. Oligonucleotide gel-based APE1 endonuclease activity assays were performed as described in Methods (8,15). The upper band (26 mer) represents uncleaved AP oligonucleotides, whereas the lower band (14 mer) is the reacted oligonucleotide. E3330, RN8-51, RN10-52, and RN7-60 had no effect on APE1 endonuclease activity. (For interpretation of the references to color in this figure legend, the reader is referred to the web version of this article at www.liebertonline.com/ars).

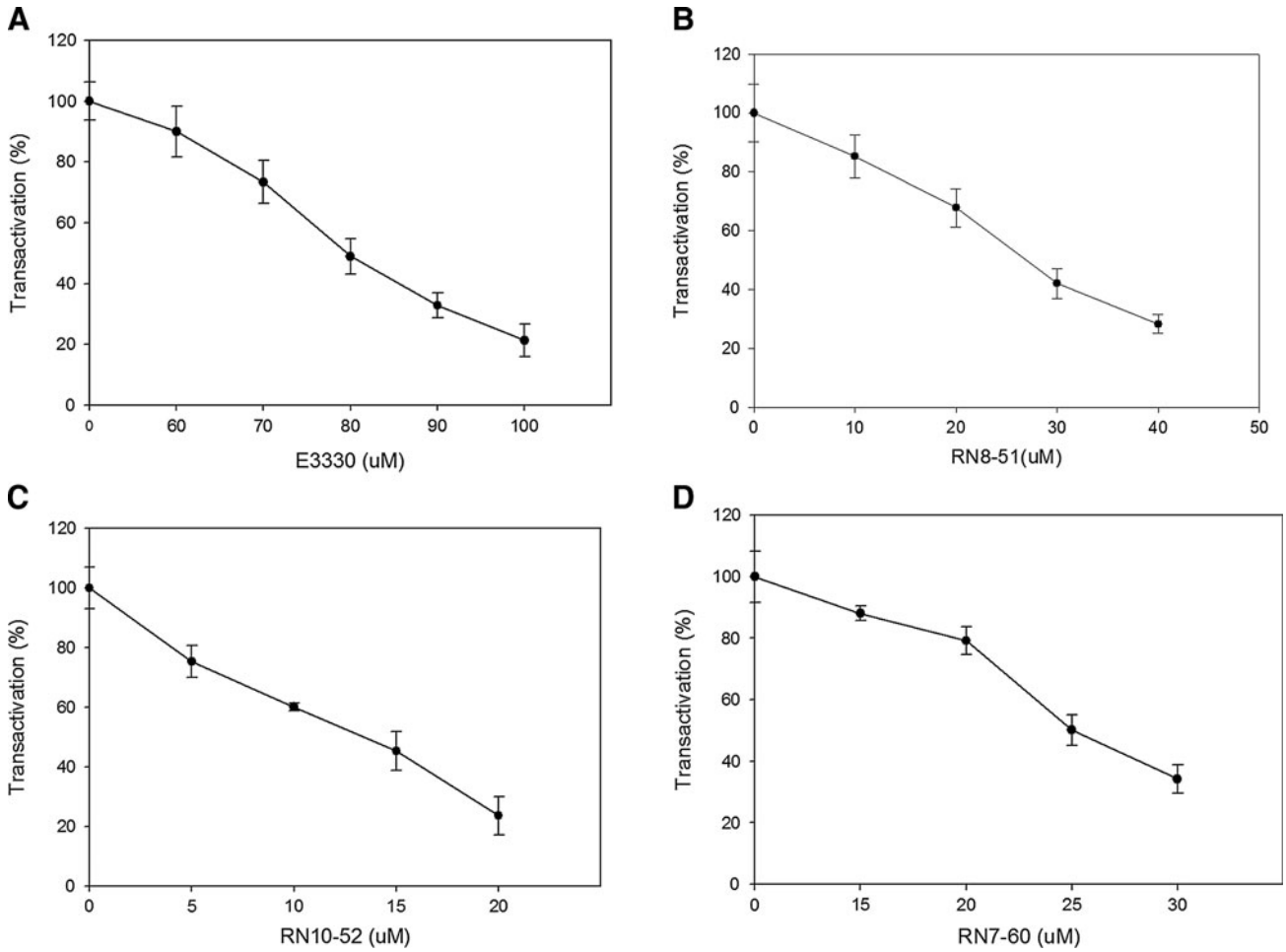

FIG. 5. E3330 analogues inhibited APE1 redox activity in transactivation assay. Increasing amounts of E3330 **(A)** or its analogues (RN8-51 **(B)**, RN10-52 **(C)**, and RN7-60 **(D)**) were added to SKOV-3X ovarian cancer cells with pNF-κB-Luc. After 40 h of treatment, luciferase activity was measured, and MTT assays were performed to measure cell numbers. The ratio of luciferase activity to MTT activity was determined to measure NF-κB activity. Data are expressed as the mean $\pm$ SEM of three independent experiments performed in duplicate and are presented as percentage transactivation compared with control of no E3330 or E3330 analogues.

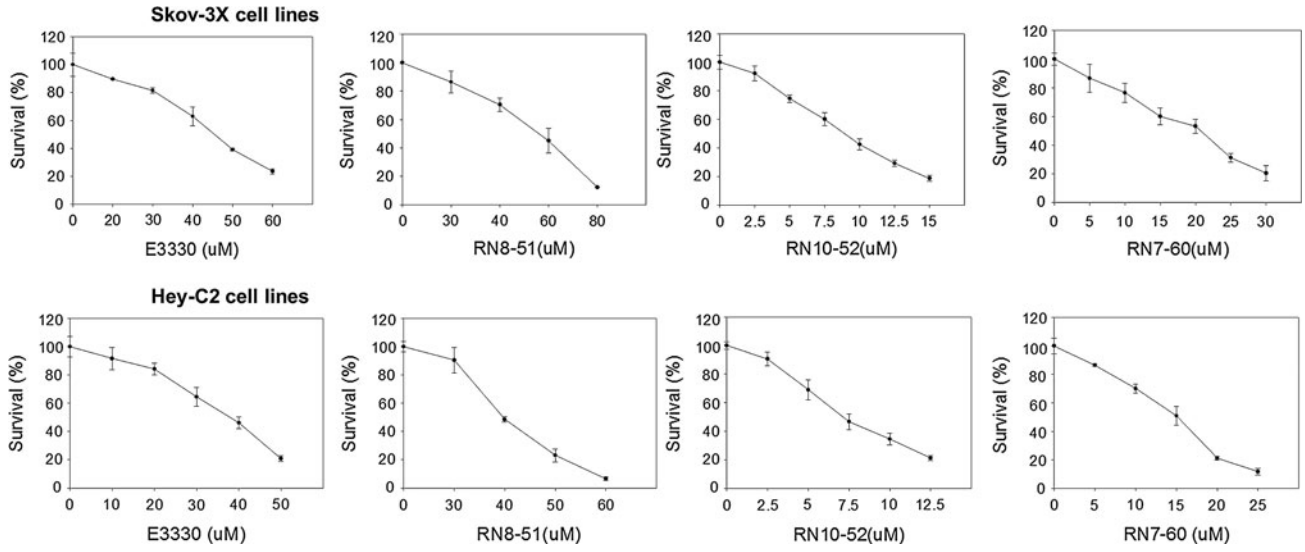

FIG. 6. Effect of E3330 analogues on cell growth/survival in two ovarian cancer cell lines. MTT assays were performed as described in Methods. Increasing amounts of E3330 and analogues resulted in decreased cell growth and decreased cell numbers in both cell lines. Analogues RN7-60 and RN10-52 had a greater effect than E3330 did; RN8-51 had an effect similar to that of E3330. Data are expressed as the mean $\pm$ SEM of three independent experiments performed in triplicate.

number of closed network units formed per well, and then normalized to the amount of closed-unit formation in the vehicle control. A significant decrease ($p < 0.001$) in closed-network tube formation was observed at 7.5 μM for E3330, 25 μM for RN8-51, 5 μM for RN10-52, and 10 μM for RN7-60–treated ECFCs (Fig. 7A and B).

Endothelial cell TUNEL assays

We also performed the TUNEL assay on ECFCs to determine the percentage of cells undergoing apoptosis. We wanted to determine whether the ablation of tube formation in this assay was due to inhibition of the tube-formation process instead of cell death. As shown (Fig. 7C), E3330 and RN8-51 did not induce any apoptosis in the cells, but hydrogen peroxide, our positive control, was very TUNEL positive. However, we did see some increase in apoptosis with RN10-52 and a dramatic apoptotic response with RN7-60. From these data, we conclude that E3330 and RN8-51 are not inducing cell killing through apoptosis.

MS analysis of the interaction of E3330 and analogues with APE1

To assess how and to what extent E3330 and its analogues react with APE1, an ESI-MS analysis was performed for a 1-min reaction of FL-APE1 and a mixture of RN7-60, RN10-52, RN 8-51, and E3330. The results were based on the assumption that the effect of modifications on the ionization efficiency is negligible. As shown in Fig. 8, covalent adducts of RN7-60 and RN10-52 with APE1 were identified in the global MS analysis, suggesting that these compounds have the highest reactivity after 1 min. The peak intensities for RN7-60– and RN10-52–modified FL-APE1 were similar (Fig. 8), suggesting that they have a similar reactivity to the protein. Modifications corresponding to one to seven additions were observed for the reactions of FL-APE1 and RN7-60 and RN10-52 after 0.5 h, respectively (Fig. 9).

After a 1-h reaction with RN8-51, about 50% and 20% of FL-APE1 was modified on single and double sites, respectively (Fig. 9). No modification of FL-APE1 by E3330 was observed

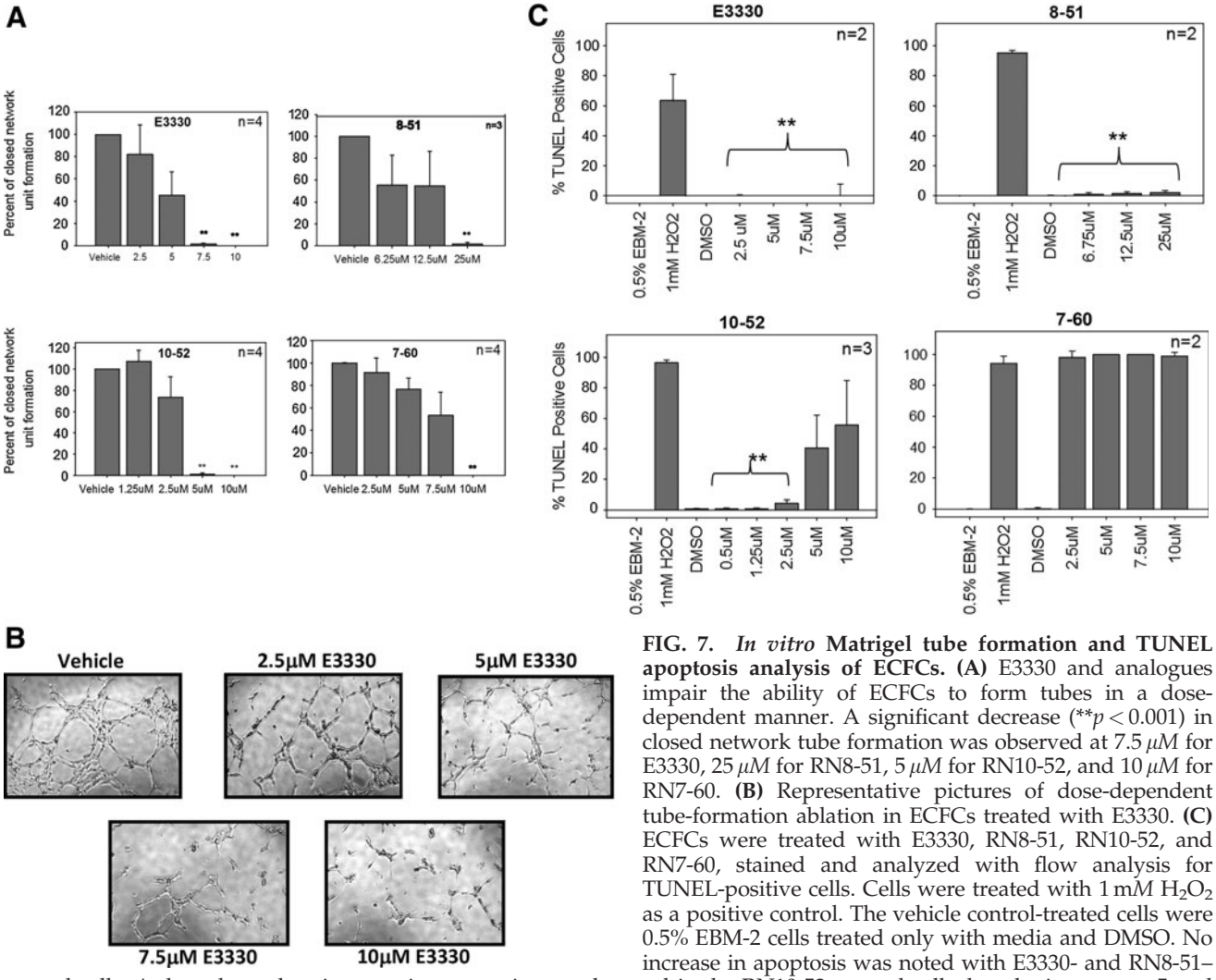

FIG. 7. ***In vitro*** **Matrigel tube formation and TUNEL apoptosis analysis of ECFCs. (A)** E3330 and analogues impair the ability of ECFCs to form tubes in a dose-dependent manner. A significant decrease ($^{**}p < 0.001$) in closed network tube formation was observed at 7.5 μM for E3330, 25 μM for RN8-51, 5 μM for RN10-52, and 10 μM for RN7-60. **(B)** Representative pictures of dose-dependent tube-formation ablation in ECFCs treated with E3330. **(C)** ECFCs were treated with E3330, RN8-51, RN10-52, and RN7-60, stained and analyzed with flow analysis for TUNEL-positive cells. Cells were treated with 1 mM H_2O_2 as a positive control. The vehicle control-treated cells were 0.5% EBM-2 cells treated only with media and DMSO. No increase in apoptosis was noted with E3330- and RN8-51–treated cells. A dose-dependent increase in apoptosis was observed in the RN10-52–treated cells, but the increase at 5 and 10 μM did not differ significantly from the vehicle control (DMSO)-treated cells. ECFCs treated with as little as 2.5 μM RN7-60 were almost entirely TUNEL positive. Statistical analysis was performed as described in Methods. ($^{**}p < 0.01$ in **C**).

after a 2-h reaction. Similar results were observed for reactions of APE1 delta 40 and E3330/analogues. After a 4.5-h reaction, APE1 delta 40 was observed with two (~24%), three (~36%), four (~28%), and five (~ 11%) modifications by RN7-60, with two (~68%) and three (~32%) modifications by RN10-52, with one modification (~32%) by RN8-51, and with no modification by E3330. The observed mass differences for peaks corresponding to adducts of RN7-60 (276 Da) and RN10-52 (319 Da) with APE1 in Figs. 8 and 9 or APE1 delta 40 correspond to mass increases of 240 Da and 283 Da, respectively, consistent with the loss of HCl (36 Da). However, the observed mass difference for RN8-51 (272 Da) adducts with APE1 or APE1 delta 40 is 274 Da, consistent with no loss of substituent moieties from RN8-51. Formation of the observed products is consistent with a Michael addition reaction, as shown in Fig. 8B. LC-MS/MS analysis of the reaction products obtained for RN7-60 and RN10-52 confirmed that these compounds covalently modify Cys residues present in APE1. However, no modified peptides were observed in the LC-MS/MS analysis of RN8-51, suggesting that the modifications of this protein are reversible.

To determine the sites of reactivity for RN8-51, APE1 delta 40 C99/138A, C99A, and C138A were reacted with RN8-51 for 3 h. These mutants were selected to determine whether RN8-51 reacts with the solvent-accessible Cys residues C99 or C138 or both. No modification was observed for the reaction with the C99A/C138A protein, one modification for C99A protein, and one modification for C138A protein (Fig. 10). Thus, we conclude that RN8-51 reacts with the two solvent-accessible cysteines C99 and C138.

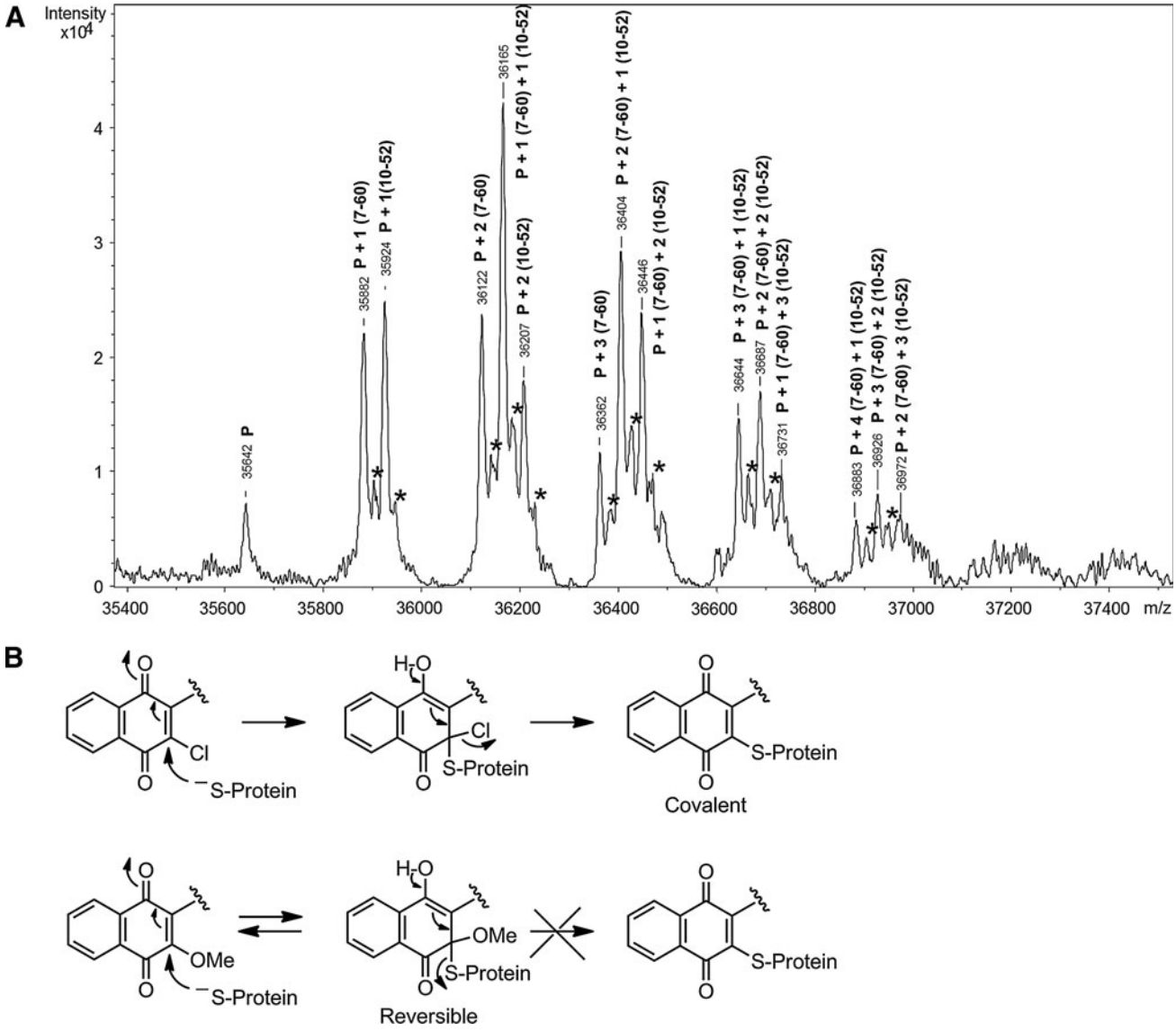

FIG. 8. ESI-MS analysis of APE1 with E3330 and analogues. (A) ESI spectra of FL-Ape1 and a mixture of ligands (RN7-60, RN10-52, RN8-51, and E3330) after 1-min reaction, showing modifications by RN7-60 and RN10-52. P, FL-Ape1; *the water adducts of the protein and ligand complexes. **(B)** Mechanism of covalent vs. reversible inhibition of APE1 redox activity.

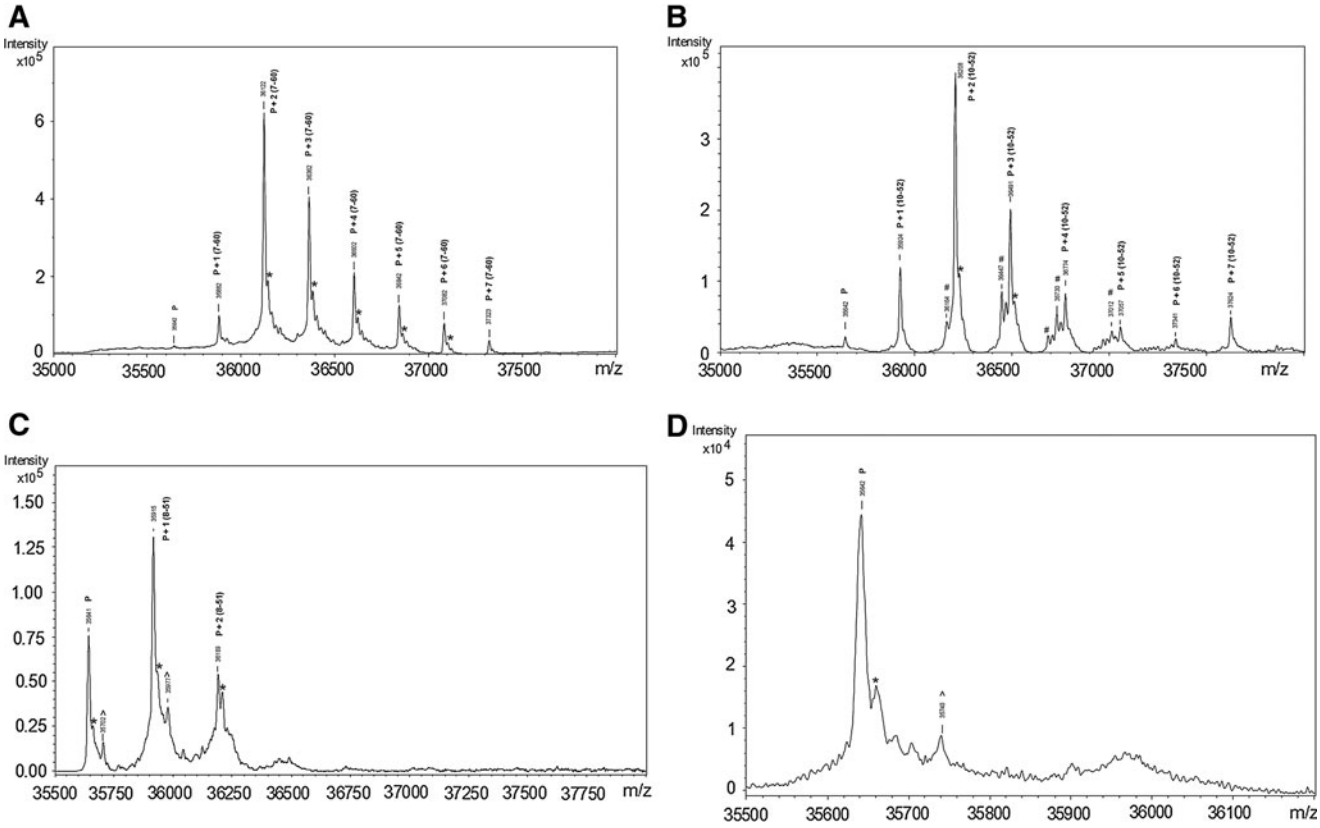

FIG. 9. ESI-MS analysis of adduct formation. (A) ESI spectra of FL-APE1 and RN7-60 after 0.5-h reaction, showing multiple (1, 2, 3, 4, 5, 6, and 7) modifications. **(B)** ESI spectra of FL-APE1 and RN10-52 after 0.5-h reaction, showing multiple (1, 2, 3, 4, 5, 6, and 7) modifications. **(C)** ESI spectra of FL-APE1 and RN8-51 after 1-h reaction, showing 1 and 2 modifications. P, FL-APE1; *the water adducts of the protein and ligand complexes; ^Unidentified peaks. **(D)** ESI spectra of FL-APE1 and E3330 after 2-h reaction, showing no modifications by E3330. P, FL-APE1; *the water adducts of the protein and ligand complexes; #contamination peaks due to the carryovers on the C18 column. ^Unidentified peaks. #Peaks correspond to a −44 from the adduct peak. This is the same loss as that going from $NH(CH_2)2OH$ to O^-, suggesting amide hydrolysis.

Discussion

We and others previously showed that E3330 specifically blocks the APE1 redox signaling function without interfering with its DNA-repair activity (17, 22). E3330 demonstrably blocks angiogenesis through APE1 inhibition both *in vitro* and *in vivo* (17, 38, 39) and affects pancreatic tumor xenograft cell growth (Fishel laboratory; unpublished data). In using selected E3330 analogues that we recently synthesized and reported (22), these studies demonstrate the activity of three additional APE1 redox inhibitors.

The overall goals of the studies presented here were to (a) identify new APE1 redox inhibitors with lower IC_{50} values than E3330, both *in vitro* and in cellular studies; and (b) use these new chemical substances to determine better how E3330 and its analogues specifically block APE1 redox function. The actual mechanism of action of APE1 redox activity has yet to be elucidated (18). As presented here, we determined that the *in vitro* redox IC_{50} of these three compounds is at least 10 times lower than that of E3330, with RN8-51 and RN10-52 in the sub-micromolar range and RN7-60 at 1.5 μM—all well below E3330 at 20 μM (Fig. 2). All of the compounds except RN7-60 were specific for APE1 redox inhibition (*i.e.*, they did not affect thioredoxin, whereas RN7-60 did), leading us to conclude that RN7-60 is not an APE1-specific redox inhibitor (Fig. 3).

An important role for the quinone moiety in this series of analogues was established through testing of the previously synthesized analogue RN7-58 (22), the dimethoxynaphthalene compound. RN7-58 did not show any inhibition even up to 100 μM (Fig. 2D). As previously stated, none of the compounds affected the AP endonuclease function of APE1, as expected (Fig. 4).

Additionally, although it was previously reported that resveratrol inhibits APE1 redox activity (34), we were unable to replicate those findings, even at resveratrol concentrations that were 5 times higher than those used previously (Fig. 2C). This finding is significant, as resveratrol is a natural compound with multiple reported activities; one is ascribed to APE1 redox inhibition (3, 33).

Finally, we determined that all three compounds blocked NF-κB activation in a dose-dependent manner, with all of the analogues having more than 3 times the inhibitory effect of E3330 in ovarian cancer cell lines (Fig. 6). Based on this cellular *in vitro* assay, these results indicate that the analogues have the potential to block APE1 redox function more efficiently than E3330 in a biologic context.

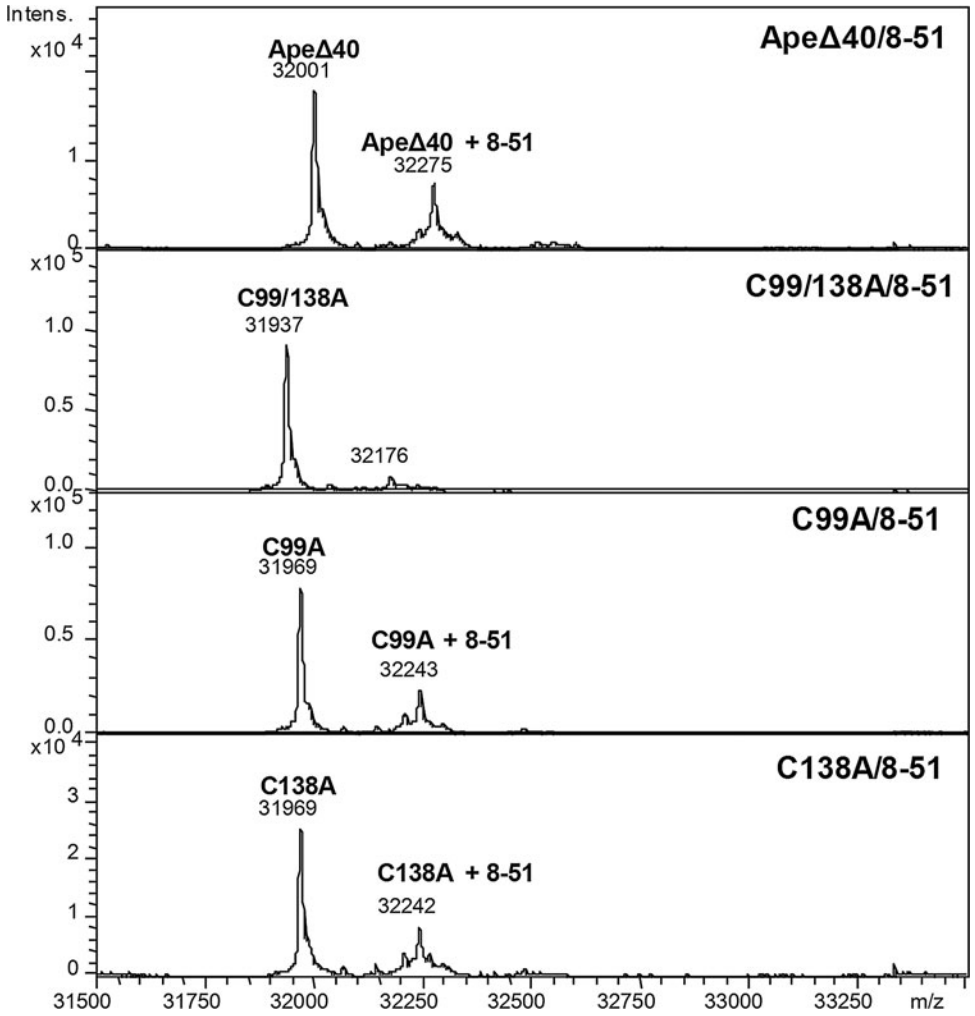

FIG. 10. ESI mass spectra of ApeΔ40 and its mutants C99A, C138A, and C99/138A after reaction with compound RN8-51. Mass spectra were collected on a Bruker MaXis UHR-TOF instrument, and deconvolution was done with the MaxEnt1 algorithm.

Although we know that APE1 plays an important role in cell growth and survival through its repair and redox functions, it is becoming apparent that the APE1 redox function is also important for angiogenesis (5, 17, 18, 38–40). We and others observed the E3330 antiangiogenesis effects (17, 38, 39). By using two angiogenesis assays, Matrigel tube formation (Fig. 7) and aortic ring-formation assays (data not shown), we observed a significant decrease in closed network tube formation, an indicator of antiangiogenic properties with all analogues, at levels similar to that observed for E3330 (Fig. 7). For RN8-51 and E3330, these results are not due to cell killing. However, RN10-52 did show some slight apoptotic effects at its higher doses, whereas RN7-60 demonstrated a dramatic apoptotic response at all doses tested. Therefore, RN8-51 appears to be the most promising of the new analogues.

Previous studies in normal dividing cells (stimulated $CD34^+$ human cells; data not shown) and in neuronal cells do not indicate that the APE1 redox function affected cell survival (8, 11, 31). However, by using two ovarian cancer cell lines, we demonstrate here that E3330 and the three analogues decrease the growth of both cell lines (Fig. 7). RN10-52 and RN7-60 have a greater effect than E3330, whereas RN8-51 has an effect similar to that of E3330. These results are consistent with the TUNEL data observed in the ECFCs and indicate that RN8-51 diminishes cell growth in cancer cell lines, as observed for E3330, but the effect is through cell-growth inhibition, not apoptosis (Fig. 7C) (5, 17, 38, 39). In contrast, some apoptosis was observed for RN10-52, whereas RN7-60 was found to induce apoptosis in nearly 100% of the cells, even at the lowest concentration used. Thus, the more-toxic effects of RN10-52 and RN7-60 are potentially problematic for *in vivo* studies, and preliminary toxicology and maximum tolerated dose (MTD) studies in mice demonstrate that RN7-60 is toxic to animals. This is not unexpected, given the promiscuous nature of RN7-60. Preliminary studies with E3330 do not show any toxicity up to 75 mg/kg, no negative pathology, and a half-life of 5.6 h in mice (data not shown).

To assess the nature of E3330 and the interactions of its analogs with, and reactivity to APE1, we conducted an ESI mass spectrometric analysis (Fig. 8). Both RN7-60 and RN10-52 reacted rapidly with APE1, forming covalent adducts through modification of Cys residues. Reacted individually,

both RN7-60 and RN10-52 resulted in +1 to +7 additions to APE1. RN8-51 was less reactive but still formed covalent adducts at levels of about 50% and 20% on single and double sites, respectively (Fig. 9).

The sites of modification by RN8-51 were either Cys^{99} or Cys^{138} or both, the two solvent-accessible Cys residues, although formation of these adducts is reversible. No covalent adducts were observed on reaction with E3330, even after a 2-h reaction. Similar results were observed when the reactions were performed with APE1 delta 40 and either E3330 or the analogues (Fig. 9). These results can be explained by the mechanism shown in Fig. 8B. Reaction of a protein thiolate with the quinone moiety generates the Michael adduct from both structures. In the cases of RN7-60 and RN10-52, the chlorine substituent provides a good leaving group, and its expulsion from the intermediate leads to the covalent adduct. In the case of RN8-51, however, the methoxy group is a poorer leaving group than the protein thiolate; the reaction reverts, and the modifications by RN8-51 are reversible.

These data led us to a number of conclusions on the mechanism of action for APE1 redox function and hypotheses concerning the interaction of APE1 with E3330 and the analogues presented in this article. Two of the analogues, RN10-52 and RN7-60, are quite reactive and readily form covalent adducts, resulting in modification not only of the two solvent-accessible but also of the five remaining interior Cys residues in APE1. These results suggest that RN7-60 and RN10-52 cause at least partial unfolding of the enzyme, exposing buried Cys residues. These two analogues were found to induce apoptosis at much higher levels than observed for RN8-51 and E3330. In contrast, RN8-51 appears to form reversible adducts with solvent-accessible Cys residues when incubated with APE1 (Fig. 10). E3330 may also react reversibly, but no adducts were observed under these conditions. Thus, we identified in this analysis a second promising APE1 redox inhibitor, RN8-51, and validated that targeting the APE1 redox activity shows promise for further translational anticancer therapeutic development.

In conclusion, the studies presented here represent additional progress toward understanding the mechanism of redox regulation of the unique multifunctional DNA-repair and redox-signaling molecule, APE1. We also show further data of biologic relevance of our laboratories' recently synthesized new and novel compounds that have anti-APE1 redox activity (22). Several significant findings have resulted from the studies presented here, indicating that (a) inhibition of the APE1 redox activity shows potential for therapeutic development, and (b) a promising new analogue of E3330 has been identified. Additionally, current work in our laboratories on the redox mechanism of APE1 is in progress, and we anticipate characterizing a novel redox mechanism based on further analysis of the interaction of E3330 with APE1.

Acknowledgments

We thank the Indiana University Simon Cancer Center angiogenesis core for help with the Matrigel and aortic ring assays. The space-filling model of E3330 was produced by courtesy of James Wikel, IU School of Medicine. This work was supported by the National Institutes of Health, National Cancer Institute [CA114571 to M.M.G., CA94025, CA106298, CA114571 and CA121168 to M.R.K.]; National Institutes of Health, National Center for Research Resources [2P41RR000954 to M.L.G]; IU Simon Cancer Center Translational initiative pilot funding [ITRAC to M.M.G. and M.R.K.]; and the Riley Children's Foundation [to M.R.K].

Author Disclosure Statement

The authors state that no competing financial interests exist.

References

1. Bapat A, Fishel ML, Georgiadis M, and Kelley MR. Going ape as an approach to cancer therapeutics. *Antioxid Redox Signal* 11: 651–668, 2009.
2. Bobola MS, Blank A, Berger MS, Stevens BA, and Silber JR. Apurinic/apyrimidinic endonuclease activity is elevated in human adult gliomas. *Clin Cancer Res* 7: 3510–3518, 2001.
3. Dudley J, Das S, Mukherjee S, and Das DK. Resveratrol, a unique phytoalexin present in red wine, delivers either survival signal or death signal to the ischemic myocardium depending on dose. *J Nutri Biochem* 20: 443–452, 2009.
4. Evans AR, Limp-Foster M, and Kelley MR. Going APE over ref-1. *Mutat Res* 461(2):83–108, 2000.
5. Fishel ML, He Y, Reed AM, Chin-Sinex H, Hutchins GD, Mendonca MS, and Kelley MR. Knockdown of the DNA repair and redox signaling protein Ape1/Ref-1 blocks ovarian cancer cell and tumor growth. *DNA Repair (Amst)* 7: 177–186, 2008.
6. Fishel ML, He Y, Smith ML, and Kelley MR. Manipulation of base excision repair to sensitize ovarian cancer cells to alkylating agent temozolomide. *Clin Cancer Res* 13: 260–267, 2007.
7. Fishel ML, Kelley MR. The DNA base excision repair protein Ape1/Ref-1 as a therapeutic and chemopreventive target. *Mol Aspects Med* 28(3-4):375–395, 2007.
8. Fishel ML, Vasko MR, and Kelley MR. DNA repair in neurons: so if they don't divide what's to repair? *Mutat Res* 614: 24–36, 2007.
9. Georgiadis M, Luo M, Gaur R, Delaplane S, Li X, and Kelley M. Evolution of the redox function in mammalian Apurinic/apyrimidinic *Mutat Res* 643: 54–63, 2008.
10. Hiramoto M, Shimizu N, Sugimoto K, Tang J, Kawakami Y, Ito M, Aizawa S, Tanaka H, Makino I, and Handa H. Nuclear targeted suppression of NF-kappa B activity by the novel quinone derivative E3330. *J Immunol* 160: 810–819, 1990.
11. Jiang Y, Guo C, Vasko MR, and Kelley MR. Implications of Apurinic/Apyrimidinic endonuclease in reactive oxygen signaling response after Cisplatin treatment of dorsal root ganglion neurons. *Cancer Res* 68: 6425–6434, 2008.
12. Kakolyris S, Kaklamanis L, Engels K, Fox SB, Taylor M, Hickson ID, Gatter KC, and Harris AL. Human AP endonuclease 1 (HAP1) protein expression in breast cancer correlates with lymph node status and angiogenesis. *Br J Cancer* 77: 1169–1173,1998.
13. Kelley MR and Fishel ML. DNA repair proteins as molecular targets for cancer therapeutics. *Anticancer Agents Med Chem* 8: 417–425, 2008.
14. Koukourakis MI, Giatromanolaki A, Kakolyris S, Sivridis E, Georgoulias V, Funtzilas G, Hickson ID, Gatter KC, and Harris

AL. Nuclear expression of human apurinic/apyrimidinic endonuclease (HAP1/Ref-1) in head-and-neck cancer is associated with resistance to chemoradiotherapy and poor outcome. *Int J Radiat Oncol Biol Phys* 50: 27–36, 2001.

15. Kreklau EL, Limp-Foster M, Liu N, Xu Y, Kelley MR, and Erickson LC. A novel fluorometric oligonucleotide assay to measure O(6)-methylguanine DNA methyltransferase, methylpurine DNA glycosylase, 8-oxoguanine DNA glycosylase and abasic endonuclease activities: DNA repair status in human breast carcinoma cells overexpressing methylpurine DNA glycosylase. *Nucleic Acids Res* 29: 2558–2566, 2001.
16. Lau JP, Weatherdon KL, Skalski V, and Hedley DW. Effects of gemcitabine on APE/ref-1 endonuclease activity in pancreatic cancer cells, and the therapeutic potential of antisense oligonucleotides. *Br J Cancer* 91: 1166–1173, 2004.
17. Luo M, Delaplane S, Jiang A, Reed A, He Y, Fishel M, Nyland II RL, Borch RF, Qiao X, Georgiadis MM, *et al.* Role of the multifunctional DNA repair and redox signaling protein Ape1/Ref-1 in cancer and endothelial cells: small molecule inhibition of Ape1's redox function. *Antioxid Redox Signal* 10: 1853–1867, 2008.
18. Luo M, He H, Kelley MR, and Georgiadis M. Redox regulation of DNA repair: implications for human health and cancer therapeutic development. *Antioxid Redox Signal* 12: 1247–1269, 2010.
19. Miyamoto K, Nagakawa J, Hishinuma I, Hirota K, Yasuda M, Yamanaka T, Katayama K, and Yamatsu I. Suppressive effects of E3330, a novel quinone derivative, on tumor necrosis factor-alpha generation from monocytes and macrophages. *Agents Actions* 37: 297–304,1992.
20. Mol CD, Hosfield DJ, Tainer JA. Abasic site recognition by two apurinic/apyrimidinic endonuclease families in DNA base excision repair: the 3′ ends justify the means. *Mutat Res* 460: 211–229, 2000.
21. Mol CD, Izumi T, Mitra S, and Tainer JA. DNA-bound structures and mutants reveal abasic DNA binding by APE1 and DNA repair coordination [corrected]. *Nature* 403: 451–456, 2000.
22. Nyland RL, Luo M, Kelley MR, and Borch RF. Design and synthesis of novel quinone inhibitors targeted to the redox function of Apurinic/Apyrimidinic endonuclease 1/redox enhancing factor-1 (Ape1/Ref-1). *J Med Chem* 53: 1200–1210, 2010.
23. Puglisi F, Aprile G, Minisini AM, Barbone F, Cataldi P, Tell G, Kelley MR, Damante G, Beltrami CA, and Di Loreto C. Prognostic significance of Ape1/ref-1 subcellular localization in non- small cell lung carcinomas. *Anticancer Res* 21: 4041–4049, 2001.
24. Puglisi F, Barbone F, Tell G, Aprile G, Pertoldi B, Raiti C, Kelley MR, Damante G, Sobrero A, Beltrami CA, *et al.* Prognostic role of Ape/Ref-1 subcellular expression in stage I-III breast carcinomas. *Oncol Rep* 9: 11–17, 2002.
25. Robertson KA, Bullock HA, Xu Y, Tritt R, Zimmerman E, Ulbright TM, Foster RS, Einhorn LH, and Kelley MR. Altered expression of Ape1/ref-1 in germ cell tumors and overexpression in NT2 cells confers resistance to bleomycin and radiation. *Cancer Res* 61: 2220–2225, 2001.
26. Shimizu N, Sugimoto K, Tang J, Nishi T, Sato I, Hiramoto M, Aizawa S, Hatakeyama M, Ohba R, Hatori H, *et al.* High-performance affinity beads for identifying drug receptors. *Nat Biotechnol* 18: 877–881, 2000.
27. Tell G, Damante G, Caldwell D, and Kelley MR. The intracellular localization of APE1/Ref-1: more than a passive phenomenon? *Antioxid Redox Signal* 7: 367–384, 2005.
28. Tell G, Quadrifoglio F, Tiribelli C, and Kelley MR. The many functions of APE1/Ref-1: not only a DNA repair enzyme. *Antioxid Redox Signal* 11: 601–620, 2009.
29. Thomson B, Tritt R, Davis M, and Kelley MR. Histology-specific expression of a DNA repair protein in pediatric rhabdomyosarcomas. *Am J Pediatr Hematol Oncol* 23: 234–239, 2001.
30. Vascotto C, Cesaratto L, Zeef LA, Deganuto M, D'Ambrosio C, Scaloni A, Romanello M, Damante G, Taglialatela G, Delneri D, *et al.* Genome-wide analysis and proteomic studies reveal APE1/Ref-1 multifunctional role in mammalian cells. *Proteomics* 9: 1058–1074, 2009.
31. Vasko MR, Guo C, and Kelley MR. The multifunctional DNA repair/redox enzyme Ape1/Ref-1 promotes survival of neurons after oxidative stress. *DNA Repair (Amst)* 4: 367–379, 2005.
32. Wang D, Luo M, and Kelley MR. Human apurinic endonuclease 1 (APE1) expression and prognostic significance in osteosarcoma: enhanced sensitivity of osteosarcoma to DNA damaging agents using silencing RNA APE1 expression inhibition. *Mol Cancer Ther* 3: 679–686, 2004.
33. Yang S, Irani K, Heffron SE, Jurnak F, and Meyskens FL. Alterations in the expression of the apurinic/apyrimidinic endonuclease-1/redox factor-1 (APE/Ref-1) in human melanoma and identification of the therapeutic potential of resveratrol as an APE/Ref-1 inhibitor. *Mol Cancer Ther* 4: 1923–1935, 2005.
34. Yang Z, Yang S, Misner BJ, Chiu R, Liu F, and Meyskens FL Jr. Nitric oxide initiates progression of human melanoma via a feedback loop mediated by apurinic/apyrimidinic endonuclease-1/redox factor-1, which is inhibited by resveratrol. *Mol Cancer Ther* 7: 3751–3760, 2008.
35. Yang ZZ, Chen XH, Wang D. Experimental study enhancing the chemosensitivity of multiple myeloma to melphalan by using a tissue-specific APE1-silencing RNA expression vector. *Clin Lymphoma Myeloma* 7(4):296–304, 2007.
36. Yuk JM, Yang CS, Shin DM, Kim KK, Lee SK, Song YJ, Lee HM, Cho CH, Jeon BH, and Jo EK. A dual regulatory role of apurinic/apyrimidinic endonuclease 1/redox factor-1 in HMGB1-induced inflammatory responses. *Antioxid Redox Signal* 11: 575–588, 2009.
37. Zhang Y, Wang J, Xiang D, Wang D, and Xin X. Alterations in the expression of the apurinic/apyrimidinic endonuclease-1/redox factor-1 (APE1/Ref-1) in human ovarian cancer and indentification of the therapeutic potential of APE1/Ref-1 inhibitor. *Int J Oncol* 35:1069–1079, 2009.
38. Zou G-M and Maitra A. Small-molecule inhibitor of the AP endonuclease 1/REF-1 E3330 inhibits pancreatic cancer cell growth and migration. *Mol Cancer Ther* 7: 2012–2021, 2008.
39. Zou GM, Karikari C, Kabe Y, Handa H, Anders RA, and Maitra A. The Ape-1/Ref-1 redox antagonist E3330 inhibits the growth of tumor endothelium and endothelial progenitor cells: therapeutic implications in tumor angiogenesis. *J Cell Physiol* 219: 2098, 2009.
40. Zou GM, Luo MH, Reed A, Kelley MR, and Yoder MC. Ape1 regulates hematopoietic differentiation of embryonic stem cells through its redox functional domain. *Blood* 109: 1917–1922, 2007.

Address correspondence to:
Dr. Mark R. Kelley
Departments of Pediatrics
Herman B. Wells Center for Pediatric Research
Walther Hall–R3
Room 528
980 West Walnut Street
Indianapolis, IN 46202

E-mail: mkelley@iupui.edu

Date of first submission to ARS Central, June 21, 2010; date of final revised submission, September 23, 2010; date of acceptance, September 26, 2010.

Abbreviations Used

AP = apurinic/apyrimidinic
APE1 = AP endonuclease 1
BER = base excision repair
CID = collision-induced dissociation
DTT = dithiothreitol
EBM = endothelial basic medium
E. coli = *Escherichia coli*
ECFC = endothelial colony-forming cell
Egr-1 = early growth response protein-1
EMSA = electrophoretic mobility shift assay
FA = formic acid
FL-APE1 = full-length APE1
FT = Fourier transform
HIF-1α = hypoxia-inducible factor 1, alpha subunit
IC_{50} = half-maximal inhibitory concentration
LC-MS/MS = liquid chromatography–tandem mass spectrometry
LD_{50} = lethal dose at 50% kill
MS/MS = tandem mass spectrometry
NF-κB = nuclear factor-κB
NF-κB Luc gene = luciferase gene with the NF-κB–responsive promoter
OD = optical density
p53 = protein 53
Redox = reduction oxidation
Ref-1 = redox effector factor 1
RVEC = retinal vascular endothelial cells
SAR = structure–activity relation
TF = transcription factor
TUNEL = TdT-mediated dUTP-fluorescein nick-end labeling